New & Renewable Energy 2024. 3 Vol. 20, No. 1
ISSN 1738-3935 (Print)
ISSN 2713-9999 (Online)
https://doi.org/10.7849/ksnre.2024.2015

[2024-3-HP-001]

Check for updates

Parametric Study of a Fixed-blade Runner in an Ultra-low-head Gate Turbine

Mohamed Murshid Shamsuddeen[1)] · Duc Anh Nguyen[2),3)] · Jin-Hyuk Kim[4),5)*]

Received 4 August 2023 **Revised** 1 November 2023 **Accepted** 12 January 2024 **Published online** 29 January 2024

ABSTRACT Ultra-low-head is an unexplored classification among the sites in which hydroelectric power can be produced. This is typically owing to the low power output and the economic value of the turbines available in this segment. A turbine capable of operating in an ultra-low-head condition without the need of a dam to produce electricity is developed in this study. A gate structure installed at a shallow water channel acting as a weir generates artificial head for the turbine mounted on the gate to produce power. The turbine and generator are designed to be compact and submersible for an efficient and silent operation. The gate angle is adjustable to operate the turbine at varying flow rates. The turbine is designed and tested using computational fluid dynamics tools prior to manufacturing and experimental studies. A parametric study of the runner blade parameters is conducted to obtain the most efficient blade design with minimal hydraulic losses. These parameters include the runner stagger and runner leading edge flow angles. The selected runner design showed improved hydraulic characteristics of the turbine to operate in an ultra-low-head site with minimal losses.

Key words Ultra-low-head, Gate turbine, Parametric study, Computational fluid dynamics, Stagger angle, Blade angle

Nomenclature

ULH : ultra low head turbines
CFD : computational fluid dynamics
RANS : reynolds-averaged navier-stokes
SST : shear stress transport
GCI : grid convergence index
LE : leading edge
TE : trailing edge
DoE : eesign of experiment
LHS : latin hypercube sampling
DV : design variable
H : head
D : runner diameter

1) Research Engineer, CFD Business Department, NineplusIT Co., Ltd.
2) Ph.D. Candidate, Industrial Technology (Green Process and Energy System Engineering, University of Science & Technology
3) Ph.D. Candidate, Carbon Neutral Technology R&D Department, Korea Institute of Industrial Technology
4) Associate Professor, Industrial Technology (Green Process and Energy System Engineering, University of Science & Technology
5) Principal Researcher, Carbon Neutral Technology R&D Department, Korea Institute of Industrial Technology
***Corresponding author:** jinhyuk@kitech.re.kr
Tel: +82-41-589-8447 Fax: +82-41-589-8330

1. Introduction

Energy from shallow waterways, also known as hydrodynamic energy, is an emerging form of renewable energy that harnesses the kinetic energy of water flowing from rivers, tides, and ocean currents. The importance of this renewable energy is rising as the globe works to lessen its reliance on fossil fuels. Due to its great efficiency, minimal maintenance requirements, and long lifespan, hydroelectricity has emerged as one of the most promising clean energy sources. Hydrodynamic systems can be deployed in shallow waterways without the need for expensive infrastructure, unlike traditional hydropower, which necessitates the construction of dams and reservoirs. Due to its low environmental effect and capacity to deliver consistent electricity, this source of energy is becoming more and more popular.

To harness kinetic energy from shallow, slow-flowing waters, Ultra Low Head Turbines (ULH) were designed. ULH turbines have a special design that makes them far more efficient and economical than conventional hydro turbines, which need high head and high flow rates to produce power. Despite the detrimental effects on the environment, hydropower is still regarded a sustainable source of renewable energy. The construction of medium- and large-scale hydropower plants is significantly hampered by environmental concerns.[1] A compact-scale hydropower sources are therefore gaining popularity since they have advantages including simplicity of deployment, compact size, and favorable environmental effect.[2] Much of the article that has been released to date focuses on hydrodynamic energy conversion technology[3,4] or small hydroelectric technology employing low heads from 3 to 30 meters.[5,6] However, water power development in scenarios with a head between 0 and 1.5 m, which is frequently referred to as ULH, has not gotten much attention due to the minimal economic benefits of resources.[7] Canals, boat locks, tidal/hydroelectric power station flows, sewage treatment plant channels, rivers and streams, marine channels, breakwaters, and other places are examples of ULH water power locations.

One of the turbines in the family of water turbines that produce power from low-pressure, high-flow water sources is the Kaplan. The adjusting mechanism of runner used by Kaplan turbine may adapt to the velocity of the water to generate as much energy as possible. Kaplan turbines also perform better under a variety of conditions since both the runner blades and guide vanes are adjustable. However, the blade adjustment mechanism is complicated and requires adequate installation space in the runner hub. Kaplan turbines are consequently more suitable for situations needing larger flow rates with lower heads due to their complexity and expense. Fixed-blade runner turbines are far more affordable and more suited for ULH applications than Kaplan turbines; nevertheless, their optimal power operating ranges are constrained.[8] A fixed-blade Kaplan turbine suitable for ULH sites with a head less than 1.5 m, efficiency more than 80% and a power output of at least 30 kW is not available in market and literatures.[9]

This study focuses on the design analysis and parametric study of a fixed-blade Kaplan turbine mounted on a gate structure suitable for ULH applications. The design analysis is conducted on an initial design and the parametric study is conducted to improve the initial design to minimize losses. The study is performed using Computational Fluid Dynamics (CFD) simulations.

2. Description of the models

The gate turbine model is designed in such a way that the water from the upstream is diverted to flow into the turbine and also to overflow above the turbine as shown in Fig. 1. A part of the incoming water is diverted into the turbine using stay vanes mounted on the gate structure. The other part is made to overflow above the gate structure such that the difference between the upstream water level and downstream water level produces the head (H) required for turbine operation. The kinetic energy of the water

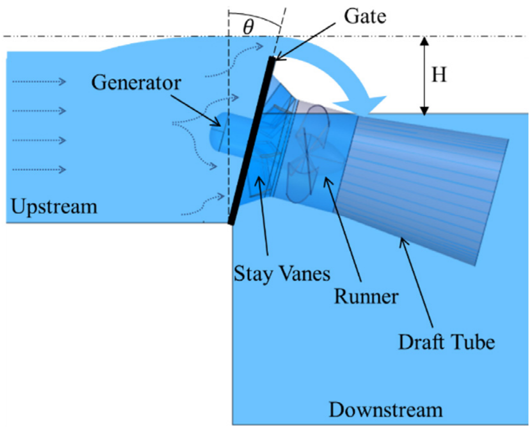

Fig. 1. Gate turbine structure and operating principle

entering the turbine is used to rotate the runner to produce electricity through the generator mounted inside the stay vanes. The kinetic energy of the remaining water is converted to gravitational potential head by the gate. The gate is mounted on a roller track and is inclinable against the upstream flow at an angle (θ) thereby controlling the head and flow rate through the turbine.

The stay vanes consisting of seven vanes ensure a uniform water distribution into the turbine by straightening the flow from the upstream channel. It maximizes the pressure energy of the water entering the turbine and also offers structural support to the generator housing. The runner consisting of three blades is the main element tasked with power extraction and energy conversion. Positioned between the stay vanes and the draft tube, the Kaplan-type runner comprises blades specially designed to harness the kinetic energy of the moving water. This energy transformation process converts the water's kinetic energy into mechanical energy, ultimately transferring it to the turbine shaft to power the electrical generator. The runner blades are fixed at a pre-determined angle such that complex governing structures inside the runner hub can be omitted thereby to reduce the manufacturing and operating costs unlike a conventional Kaplan runner. As a reason, it is important to find the most efficient blade angle prior to manufacturing the turbine. This is obtained through parametric study of the runner shape parameters including the blade angle and the stagger angle and is presented in this paper. The specifications of the turbine are provided in Table 1.

Table 1. Specifications of the turbine

Description	Value
Runner Diameter	D
Shroud radius	D/2
Number of runner blades	3
Number of stay vanes	7
Runner length	0.6D
Gate height (h_{gate})	1.81D
Inclination Angle (θ)	10 – 20°
Head (H)	1.1m

3. Numerical Model

Utilizing the computer, CFD[10] expands the capability of fluid mechanics analysis. The skilled engineer can use CFD to provide cost-effective, precise predictions that are very insightful and flexible. The analytical procedure is made much simpler with the assistance of CFD. The ANSYS software is utilized in the current study to examine the internal flow characteristics and determine the efficiency of the turbine model. The steady RANS equations for 3D incompressible flow are used to perform the numerical analysis. The finite volume approach is used to discretize these governing equations.

$$\frac{\partial \rho}{\partial t}+\frac{\partial(\rho u_i)}{\partial x_i}=0 \tag{1}$$

$$\rho\left[\frac{\partial(u_i)}{\partial t}+\frac{\partial(u_i u_j)}{\partial x_j}\right]=-\frac{\partial \rho}{\partial x_i}+\frac{\partial}{\partial x_j}\left[\mu\frac{\partial u_i}{\partial x_j}-\rho\overline{u'_i u'_j}\right] \tag{2}$$

where $-\rho\overline{u'_i u'_j}$, ρ, t, u_i, μ, and p denote the Reynolds stress, fluid density, time, fluid velocity components, turbulent eddy viscosity, and local static pressure strength, respectively.

The shear stress transport (SST $k-\omega$) turbulence model established by Menter,[11] which is utilized as a turbulence closure model in this work, is used to get an understanding of the internal flow taking place inside the turbine. The SST turbulence model uses the advantages of $k-\omega$ and $k-\varepsilon$ models with a blending function which makes a good transition between them.[12,13] The $k-\omega$ turbulence model captures the flow field happening at near-wall surfaces while the $k-\varepsilon$ turbulence model is used for the bulk flow region to analyze the turbulence. The wall function is automatically employed in the calculating procedure for a smooth transition between these two turbulent models.

3.1 CFD model and boundary conditions

The turbine performance is analyzed using numerical solver solving for the governing and turbulence equations. Numerical fluid domains are created and meshed for the simulation. An inlet domain, a runner domain and a draft domain are generated. Except for the runner, all other components of the turbines are defined as stationary domains. The General Grid Interface method transfers data between rotating and stationary domain boundaries, utilizing stage (mixing plane) interfaces. The inlet is defined as a pressure inlet with corresponding turbine head pressure, and the outlet as a mass flow outlet with specific mass flow rate. Walls are assigned automated wall functions and a no-slip boundary condition. The boundary conditions are given in Fig. 2.

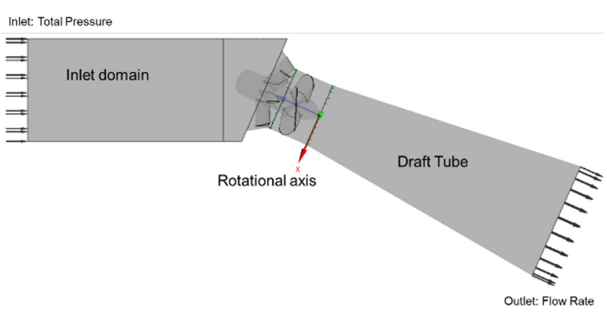

Fig. 2. Numerical domains and boundary conditions

3.2 Grid Independency Test (GCI)

Grid independence test is vital for precise fluid domain simulations. Numerical grids were constructed using tetrahedral meshing for complex stationary domains using ANSYS meshing tools, while ANSYS TurboGrid was used for runner blades, and stay vane meshes. Multi-layered prism mesh employed at the runner surfaces ensured boundary layer resolution and adherence to orthogonal quality and aspect ratio guidelines. Grid independence was assessed with the Grid Convergence Index (GCI), a reliable Richardson extrapolation-based method.[14] Three grids with resolutions of 2.98 million, 1.7 million, and 0.7 million were examined for the key variable (Power Output). The GCI values between lower and higher grids were 0.26 and 0.15, respectively. The finest grid yielded the lowest GCI value, confirming its optimality and eliminating the need for further mesh refinements.

4. Results and Discussions

4.1 Validation

The initial gate turbine model is an improved design of turbine developed by Park *et al.* (2018)[15] for power production in a marine waterway. The turbine development involved several stages. Firstly, the CFD model is validated with the experimental results of Park *et al.* (2018)[15]. Secondly, the runner profiles, stay vane profiles, and draft tube shape are extracted and scaled to the required size for an ultra-low-head site. An

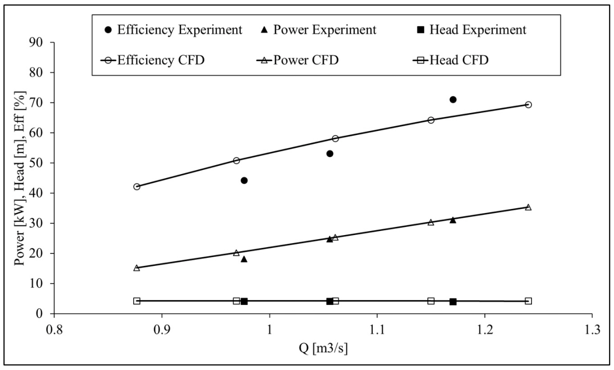

Fig. 3. Validation of the numerical model with the experimental data of Park *et al.* (2018)[15]

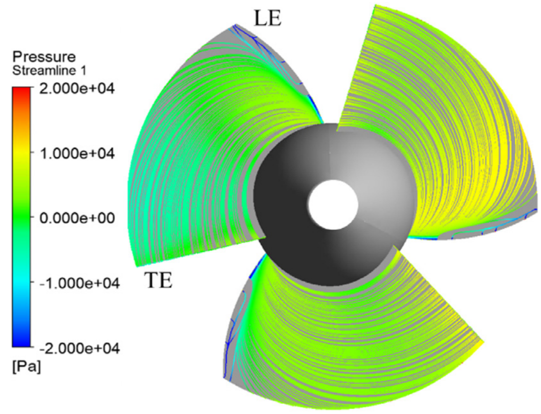

Fig. 4. Velocity streamline distribution at runner suction side colored by pressure

additional movable gate component is introduced to create an artificial head. Finally, the gate turbine model is developed with additional structural supports.

For the purpose of validation of the numerical model, the CFD model of Park's turbine is created and tested using the same boundary conditions. Fig. 3 shows the comparison of the hydraulic parameters of the turbine. The power and head obtained from the steady model have a relative error of less than 4% while the efficiency has a relative error of 5% compared to the experimental results. The CFD model's validation shows reasonable agreement with experimental results.

4.2 Initial model performance

The initial geometry of the gate turbine inspired from its predecessor is developed and simulated using a new CFD model to obtain the turbine performance at the proposed site. The boundary conditions are obtained from the site and from the results of our previous study.[16] The initial turbine model produced a power output of 40.09 kW at a head of 1.16 m, rotation speed of 123 rpm and at a flow rate of about 4 m^3/s. The efficiency of the turbine was obtained at 86.4%. The internal characteristics of the turbine are examined using the post processing tool to visualize the flow behavior at the runner blades.

Fig. 4 shows the velocity streamlines distribution along the suction side of the runner colored by the pressure at the blade surface. It can be noted that, at the leading edge (LE) of the runner, a flow separation is observed for all the three blades. The pressure falls below the ambient pressure leading to formation of a low-pressure zone at the leading edge. The low-pressure zone contributes to runner losses by decreasing its capability to convert energy efficiently. This is quantitatively estimated by plotting the blade loading distribution along the blade surface at the hub, mid and shroud spans in Fig. 5. The pressure at the LE (Streamwise 0) drops to a low value for the shroud span followed by the mid span. The pressure

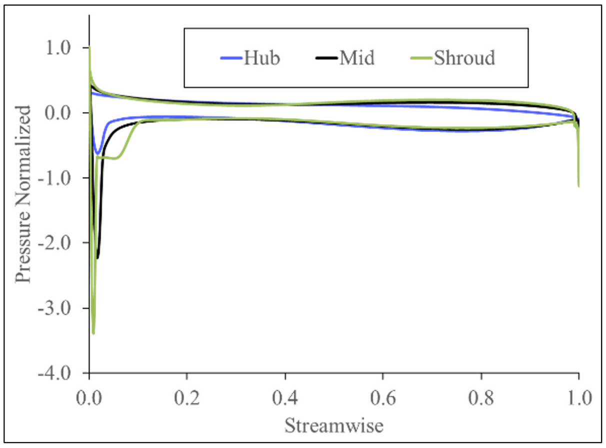

Fig. 5. Blade loading distribution of the initial turbine model

drop is also observed at the trailing edge at the shroud span however the magnitide at leading edge is higher than at the trailing edge.

The long-term effect of such low-pressure zones is the formation of cavitation bubbles and finally leading to cavitation damage on the blade surface thereby decreasing the lifespan of the turbine blade. In order to address this issue, the runner shape parameters must be corrected by conducting a parametric study on the runner inlet angles. Firstly, the runner stagger angle was studied for the mid and shroud span with a range of ±5%. Secondly, the runner leading edge beta angle was studied for the mid and shroud span by modifying the beta angle curve. The hub span is unchanged as flow losses are not observed at this location.

4.3 Parametric study

4.3.1 Runner Stagger Angle

The variables chosen for the parametric study are the runner stagger angle and runner beta angle.[17] The stagger angle is varied by a range of 5% towards the clock-wise and anti-clockwise by pivoting at the center of the blade. A design of experiment (DoE) technique is employed to generate several design samples of the blade. A sample space of 12 designs is created by a combination of stagger angle values at the mid and shroud spans. The sample space is generated using the Latin Hypercube Sampling (LHS) technique. LHS generates random samples within the design space, ensuring it meets space-filling requirements. The quantity of samples produced by LHS is not dependent on the number of design variables. LHS is valuable for concentrating these samples effectively within the design space, resulting in accurate predictions of interactions within the given space. Fig. 6 shows the LHS samples generated for the variables. The normalized values of the stagger angle are given in Table 2.

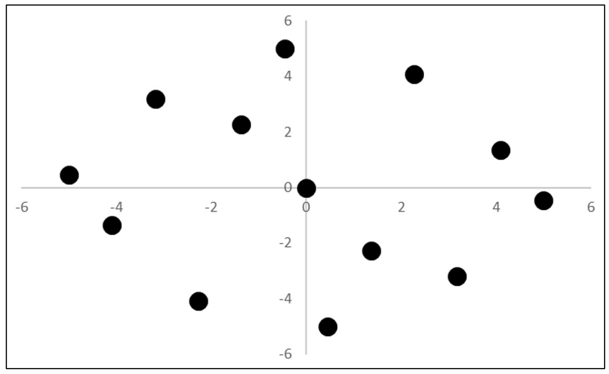

Fig. 6. LHS sampling points for stagger angle

Table 2. Stagger angle samples for mid and shroud spans

Case	Mid	Shroud
Reference	0	0
1	−4.0909	−1.3636
2	−1.3636	2.2727
3	−2.2727	−4.0909
4	−0.45455	5
5	5	−0.4545
6	3.1818	−3.1818
7	−3.1818	3.1818
8	−5	0.4545
9	0.4545	−5
10	2.2727	4.0909
11	1.3636	−2.2727
12	4.0909	1.3636

4.3.2 Runner Leading Edge Beta Angle

Two control points on the leading edge of the runner beta angle distribution profile are chosen at the mid and shroud spans. The design variables marked in green for optimization are illustrated in Fig. 7. Bezier curves, which are smooth curves defined by control points, are used to shape the profile curve between two endpoints. To limit the number of design variables, the chosen design variables are adjusted solely along the vertical axis. A total of 4 design variables are chosen. The sample space is generated using the DoE technique, 2^k factorial. Factorial design is a widely used DoE technique that generates sample points precisely at the design space boundaries. Through statistical analysis, the main effects and interactions between variables can be assessed. The 2^k factorial design is particularly effective in providing accurate predictions at the edges of the design space. A total of 8 samples are generated for the 4 design variables and their normalized values are given in Table 3. The angles are varied by ±5% where +1 indicates +5% change and −1 indicates −5% change.

The hydraulic characteristics of the samples generated through the two parametric studies are plotted using

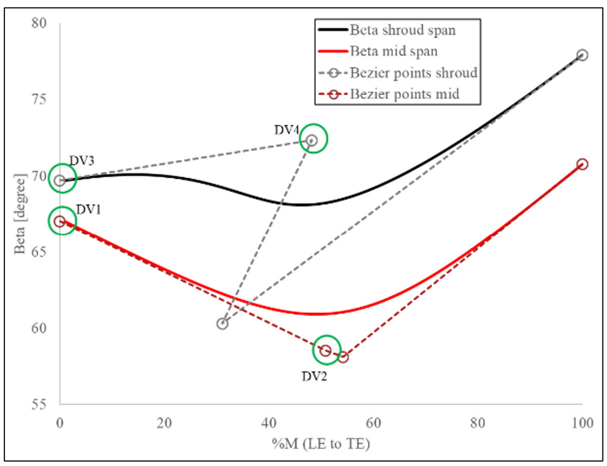

Fig. 7. Runner leading edge beta angle distribution and the selected Bezier points

Table 3. Leading edge beta Bezier points at the mid and shroud span

Case	DV1	DV2	DV3	DV4
1	−1	−1	1	1
2	−1	1	1	−1
3	−1	1	−1	1
4	1	−1	1	−1
5	1	−1	−1	1
6	1	1	−1	−1
7	1	1	1	1
8	−1	−1	−1	−1

efficiency vs power curve in Fig. 8. The variables are normalized by the reference values. The stagger angle parameter (P1) has widespread range of outputs ranging from large power outputs to high efficiency. The highest power output was obtained at an increase of 32.47% for the Parameter 1, case 5 (P1,5). However, the large power output comes at a cost of decreased efficiency by 3.3%. The highest efficiency of the P1 designs is obtained at 0.97% (P1,3) higher than reference model. The beta angle parameter (P2) shows better performance than P1 designs. Two designs namely, P2,8 and P2,3 shows higher efficiency of 1.56% and 1.35%, respectively. The power output of these designs is −15.56% and +3.6%, respectively. The rest of the designs fall within the visible range.

The lowest performing designs are (P1,8 and P1,9) with decrease in both power as well as efficiency. Interestingly, the stagger angle of both these designs is towards the −5° boundary. The stagger angle parameter aided in finding the design with high power output but produced only two high-efficiency designs high efficiency design. Comparatively, the beta angle parameter produced 6 high efficiency designs with a maximum efficiency of 87.74%. Therefore, it can be inferred that the parameter 2 outperformed parameter

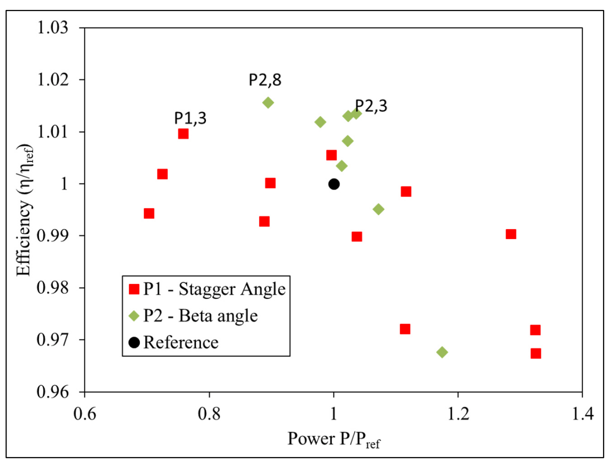

Fig. 8. Efficiency vs Power curve of the two parameters

1 in terms of producing efficient runner designs. In order to decide on the best runner design, the internal flow characteristics of the designs P2,8 and P2,3 are studied and compared with the reference model.

The blade loading distribution of the selected designs is shown in Fig. 9. The P2,8 model exhibits a decreased pressure value at the leading edge at all the three spans while the P2,3 model shows a slightly larger pressure value at the leading edge at the mid and shroud spans. However, compared to the reference runner blade, the low-pressure zone has been decreased significantly in both the models. In the P2,8 model, the pressure curve for the remaining streamwise direction shows lower area between the pressure side and suction side of the blade at all spans. The lower the area under the blade loading curve, the lower the power output from the runner. This is also observed previously with a 15.56% decrease in power output by the P2,8 design. In the case of P2,3 model, the area between the pressure curves is larger than both reference and P2,8 designs thereby producing an increased power output of 3.6%.

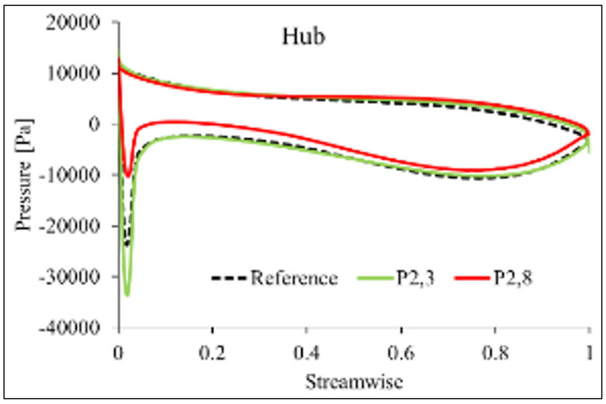

(a) Hub span

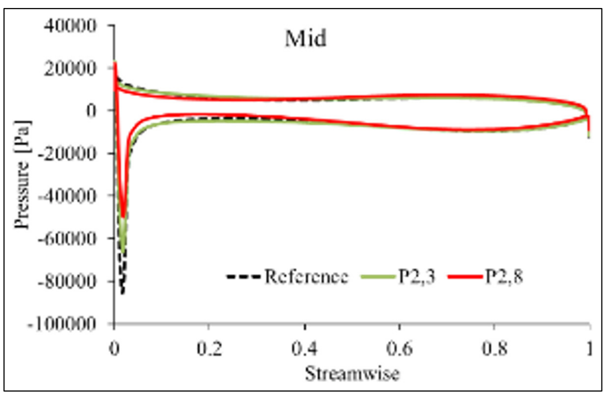

(b) Mid span

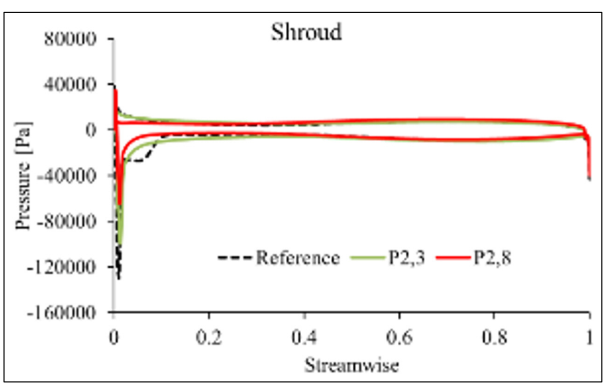

(c) Shroud span

Fig. 9. Blade loading distribution comparison of the selected designs

The velocity streamlines along the runner suction side colored by pressure are compared for the selected models in Fig. 10. The large pressure drop is observed at the leading edge of the runner in the reference model is virtually diminished in the P2,8 model and P2,3 models. This is due to the flow correction occurring by adjusting the blade beta angle. The velocity streamlines appear to be smooth curves as compared with the reference model thereby decreasing any flow separation at the runner leading edge. Therefore, it can be said that the parametric study, especially parameter 2 aided in obtaining a better runner design with fewer losses.

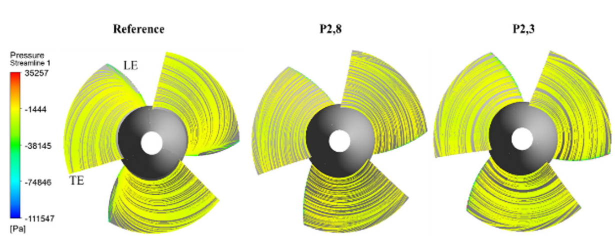

Fig. 10. Streamlines on runner surface colored by pressure for the selected models

5. Conclusions

A hydro turbine suitable for electricity production from ultra-low-head sites is designed and tested using computational fluid dynamics simulations. The initial geometry is extracted from a similar turbine and modified to suit to the ULH requirement of the proposed test site. A 3-bladed axial turbine with a Kaplan-type fixed runner along with stay vanes and a draft tube are mounted on a hydraulic gate structure that is capable of moving between a range of inclination angles against the incoming flow. A generator is installed inside the stay vane hub fully submerged in the water making the turbine a compact turbine easy for installation and transportation. The initial design was tested using CFD simulations in a previous study to obtain the initial turbine performance. Pressure losses were observed at the runner suction side at the leading edge thereby calling for a parametric study on the runner shape parameters. A parametric study involving the runner stagger angle and runner inlet beta angle were studied and the results are presented in this paper. The boundary conditions required for the parametric study stated in this paper were obtained from the previous study. Two design variables for the stagger angle parameter and four design variables for the beta angle parameter were chosen for the study. Two design of experiment techniques, namely Latin Hypercube Sampling and 2^k factorial designs were employed to generate the sample space for the study. A total of 12 samples were generated for LHS and 8 samples for 2^k partial factorial designs. Steady state numerical simulations were conducted on these selected samples and the performance of the turbine was calculated based on the head, flow rate, power output and hydraulic efficiency. The stagger angle parameter succeeded in generating runner designs with high power output but at low efficiencies. It was observed that beta angle parameter had higher influence on the turbine characteristics thereby producing high efficiency designs. The pressure losses at the runner suction side leading edge were decreased by 41.5% and 24.6% for the mid and shroud span respectively. As a result, the turbine efficiency improved by 1.56%. The gate turbine shows a promising technology with a high efficiency and power output suitable for ULH applications.

Acknowledgment

This work was supported by the Korea Institute of Energy Technology Evaluation and Planning (KETEP) grant funded by the Ministry of Trade, Industry and Energy, South Korea (MOTIE) (20217410100010, Development on the Unused Energy Utilization Technology for Medium and Large CHP Cooling Tower).

References

[1] Burke, M., Jorde, K., and Buffington, J.M., 2009, “Application of a hierarchical framework for assessing environmental impacts of dam operation: Changes in streamflow, bed mobility and recruitment of riparian trees in a western North American river”, J. Environ. Manage., **90**(SUPPL. 3), S224-S236.

[2] Kumar, D., and Katoch, S.S., 2015, “Small hydropower development in western Himalayas: Strategy for faster implementation”, Renew. Energy, **77**, 571-578.

[3] Güney, M.S., and Kaygusuz, K., 2010, “Hydrokinetic energy conversion systems: A technology status review”, Renew. Sustain. Energy Rev., **14**(9), 2996-3004.

[4] Yuce, M.I., and Muratoglu, A., 2015, “Hydrokinetic energy conversion systems: A technology status review”, Renew. Sustain. Energy Rev., **43**, 72-82.

[5] Loots, I., Dijk, M.V., Barta, B., Vuuren, S.J.V., and

Bhagwan, J.N., 2015, "A review of low head hydropower technologies and applications in a South African context", Renew. Sustain. Energy Rev., **50**, 1254-1268.

[6] Paish, O., 2002, "Small hydro power: technology and current status", Renew. Sustain. Energy Rev., **6**(6), 537-556.

[7] Shimokawa, K., Furukawa, A., Okuma, K., Matsushita, D., and Watanabe, S., 2012, "Experimental study on simplification of Darrieus-type hydro turbine with inlet nozzle for extra-low head hydropower utilization", Renew. Energy, **41**, 376-382.

[8] Zhou, D., and Deng, Z.(Daniel), 2017, "Ultra-low-head hydroelectric technology: A review", Renew. Sustain. Energy Rev., **78**, 23-30.

[9] Shamsuddeen, M.M., 2023, "Design analysis and performance enhancement of hydraulic turbines with a Kaplan-type runner using computational fluid dynamics", Ph.D., University of Science and Technology(UST), Daejeon.

[10] Date, A.W., 2005, "Introduction to computational fluid dynamics", Cambridge University Press, United Kingdom.

[11] Menter, F., 2009, "Innovative turbulence modeling: SST Model in ANSYS CFX".

[12] Shahzer, M.A., Kim, S.J., Cho, Y., and Kim, J.H., 2022, "Suppression of vortex rope formation and pressure fluctuation using anti-swirl fins in a Francis turbine model at part load condition with cavitation inception point", Phys. Fluids, **34**(9), 097106.

[13] Shahzer, M.A., Cho, Y., Shamsuddeen, M.M., and Kim, J.H., 2023, "Investigation of cavitating vortex rope instabilities and its suppression inside a Francis turbine model with Thoma number variation", Phys. Fluids, **35**(3), 033310.

[14] Celik, I.B., Ghia, U., Roache, P.J., Freitas, C.J., Coleman, H., and Raad, P.E., 2008, "Procedure for estimation and reporting of uncertainty due to discretization in CFD applications", ASME. J. Fluids Eng., **130**(7), 0780011-0780014.

[15] Park, N., Rakibuzzaman, M., and Suh, S.H., 2018, "Flow analysis of 30 kW gate turbine using permanent magnetic generator", Heat Transf. Eng., **40**(17-18), 1511-1522.

[16] Shamsuddeen, M.M., Ma, S.B., Park, N.H., Kim, K.M., and Kim, J.H., 2023, "Design analysis and optimization of a hydraulic gate turbine for power production from ultra-low head sites", Energy, **275**, 127371.

[17] Kim, J., Suh, J., Kim, J., Choi, Y., Lee, K., and Kim, J., 2017, "Effect on the efficiency of a counter-rotating pump-turbine with the variation of blade angle using design of experiment (2^k factorial design)", New. Renew. Energy, **113**(1), 17-26.